

Application of Wedge Diffraction Theory to Estimating Power Density at Airport Humped Runways

ALFRED R. LOPEZ, FELLOW, IEEE

Abstract—Shadowing caused by humped runways at some airports significantly attenuates the guidance signals of the microwave landing system as the aircraft approaches the touchdown point. Application of wedge diffraction theory provides an estimate of this effect. A wedge diffraction factor is presented which relates the signal strength in the shadow to that for line-of-sight on a flat runway. Computations are confirmed by measurements at two airports.

I. INTRODUCTION

AIRCRAFT LANDING guidance systems use antennas sited beyond the stop end of the runway to radiate the azimuth guidance and distance measuring signals. Runways where the line-of-sight is blocked between the transmitting antennas and the landing threshold have been referred to as "humped" runways. The determination of the radiated power density in the shadow is important with respect to the requirements for automatic landing. The microwave landing system (MLS) is now entering a world-wide transition phase. The transition plan is that by the year 2000, all instrument landing systems (ILS) would be withdrawn as an International Civil Aviation Organization requirement, and the MLS would be universally installed. It is important that guidelines for installing the ground equipment and predicting power density levels be established early in the transition phase.

Analytic studies of the shadowing effects caused by a humped runway have provided estimates of the attenuation in the shadow region. Lincoln Laboratory [2] has used the Wait-Conda solution of diffraction by a cylinder [3] to estimate the signal attenuation in the shadow. It is believed that the model presented in this paper is better suited for estimating the power density for the humped runway situation.

Wedge diffraction is a classic electromagnetic field problem [1] which has a rigorous solution. It is well suited for application to the humped runway situation since most runways are constructed such that the runway centerline can be approximated by a few straight line segments. The wedge diffraction model can provide an estimate of the signal level along the aircraft approach path to a runway. It will predict power density levels during the initial and final phases of the approach, including touchdown and rollout. It will also predict power density for the case of a flat runway and for the case of an inverted hump.

The application of wedge diffraction theory to the problem of estimating power density for the case of a humped runway was first attempted by the United Kingdom Royal Aircraft Establishment [4]; however, as noted in [2] the approach implemented did not yield acceptable results. More recently, workers using geometrical diffraction theory have shown the wedge to be a very useful model in predicting terrain propagation effects [5], [6], [7]. The model presented in this paper uses the concepts of geometrical diffraction [8]. It provides estimates of the humped runway effects using simple functions to approximate the characteristic Fresnel integrals. These approximate functions simplify the computations.

II. PROBLEM DEFINITION

To get a perspective of the problem, an actual airport runway situation is described. Runway 14 at Ottawa International Airport, Canada, has a pronounced hump as shown in Fig. 1. An MLS azimuth angle guidance station [9] is located beyond the stop end, with the data antenna phase center located as shown in the figure.

The MLS angle guidance equipment uses several antennas to radiate the required time-division-multiplex signal-in-space. One of these antennas is called the data antenna. This antenna radiates a differential phase-shift keying (DPSK) modulated signal throughout the coverage volume such that a receiver can identify which angle guidance function (azimuth or elevation) is being transmitted. The radiation is vertically polarized. The data antenna is used in this analysis because it is a passive antenna, its gain and pattern characteristics are well established and it should be close to universal for all equipments.

The vertical field strength pattern for this antenna has a slope at the horizontal of 8 dB/degree [10]. This pattern is a sector pattern which extends from 0° to about 20° in elevation and has sidelobes below the horizontal that are more than 14 dB below the pattern peak. For the purposes of this analysis, only the cutoff characteristic at the horizon is of interest. This particular pattern characteristic is approximated by the expression

$$V(\theta) = 1 + 0.8 \tanh(A\theta) \quad (1)$$

where

θ = angle above the relevant shadow boundary (in degrees, Fig. 2 defines θ for the transmitter)

Manuscript received June 3, 1986; revised January 2, 1987.
The author is with Hazeltine Corporation, 500 Commack Road, Commack, NY 11724.
IEEE Log Number 8714658.

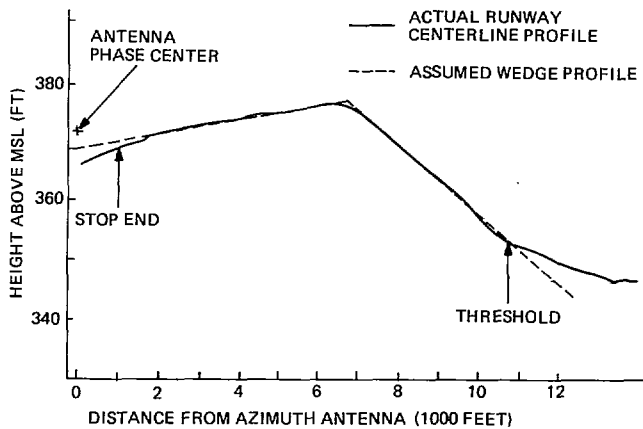


Fig. 1. Ottawa runway 14 centerline profile.

$$A = 1.215 \text{ (rad/degree).}$$

The data antenna has the following characteristics:

$$\begin{aligned} G &= \text{gain in the shadow boundary direction} = 8 \text{ dBi} \\ P &= \text{transmitter available power} = 13 \text{ dBW (20 W)} \\ \lambda &= \text{wavelength} = 0.06 \text{ m (0.2 ft)}. \end{aligned}$$

The problem is to predict accurately the power density radiated by the antenna along the aircraft approach path, including the segment through the shadow region. A wedge surface is used to approximate the runway surface as shown in Fig. 1 for application to prediction of the power density. For the purpose of this paper it is assumed that the ground reflection coefficient for the vertically polarized signal is -1 . This is a good approximation. The reflection coefficient for ground surfaces approaches -1 as the grazing angle approaches zero and is less than the Brewster angle (say less than 3°).

III. WEDGE DIFFRACTION MODEL

The geometry for the wedge diffraction model is shown in Fig. 2. The figure defines distances and angles. As shown in the figure, the signal at the receiver is the sum of direct, reflected and diffracted signals. The reflected signal in general consists of two components. In some cases only one reflected component exists. For the case of $\alpha + \beta < \pi/8$ (i.e., small deviation from flat ground case) the diffracted signal can be closely approximated by four components. The transmitter and the three images shown in Fig. 2 excite these dominant diffraction components. Each diffraction component has maximum amplitude in the direction of the corresponding shadow boundary [11]. In (2), (3), and (4) the field strengths are relative to the free space field strength at the shadow boundary at a distance of $D1 + D2$.

The direct field strength $E1(\theta)$ is given by

$$E1(\theta) = \frac{D1 + D2}{D3} V(\theta) u(\theta) \exp\left(j \frac{2\pi}{\lambda} (D1 + D2 - D3)\right) \quad (2)$$

where

$$\begin{aligned} u(\theta) &= 1, \quad \theta \geq 0 \\ &= 0, \quad \theta < 0. \end{aligned}$$

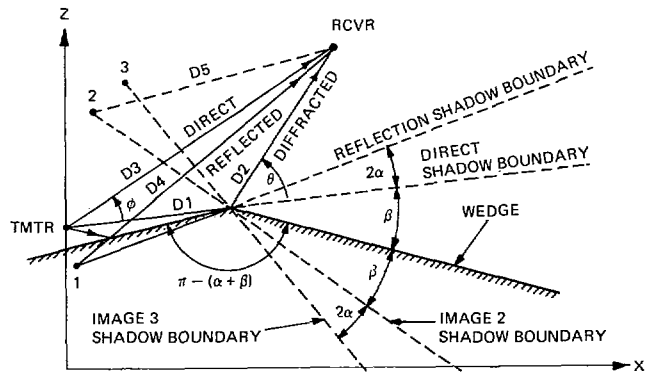


Fig. 2. Wedge diffraction geometry.

The reflected field strength $E2(\theta)$ is given by

$$\begin{aligned} E2(\theta) &= \frac{D1 + D2}{D4} V'(\theta - 2\alpha) u(\theta - 2\alpha) \\ &\quad \cdot \exp\left(j \frac{2\pi}{\lambda} (D1 + D2 - D4)\right) \\ &\quad + \frac{D1 + D2}{D5} V'(\theta + 2\beta) u(-\theta - 2\beta) \\ &\quad \cdot \exp\left(j \frac{2\pi}{\lambda} (D1 + D2 - D5)\right) \quad (3) \end{aligned}$$

where

$$V'(\theta) = 1 - 0.8 \tanh(A \theta).$$

The diffracted field strength $E3(\theta)$, which can be expressed rigorously in terms of a Fresnel integral for the case of $D1$ and $D2 \gg \lambda$, and $\alpha + \beta < \pi/8$ is given by a simple approximation. (It is recalled that in the illuminated region the Fresnel integral has an oscillatory component. The oscillation is caused by the phase variation of the diffracted signal with respect to the direct signal. In the illuminated region, the diffracted signal expressed below is in terms of a Fresnel integral minus the direct signal.)

$$\begin{aligned} E3(\theta) &= \left(\frac{\tanh(v)}{2v} - \frac{v}{4} \exp(-1.5v) \right) \text{sgn}(\theta) \\ &\quad \cdot \exp\left(-j \frac{\pi}{4} \tanh(v/2.4)\right) \quad (4) \end{aligned}$$

where

$$v = 2\pi\sqrt{D/\lambda} |\sin(\theta/2)|$$

$$D = \frac{(D1)(D2)}{D1 + D2}$$

$$\begin{aligned} \text{sgn}(\theta) &= 1, \quad \theta \geq 0 \\ &= -1, \quad \theta < 0. \end{aligned}$$

For $v = 0$, $E3(0) = 1/2$; for large v ($v > 2\pi$), $E3(\theta)$ approaches

$$E3(\theta) = \frac{\exp(-j\pi/4)}{2v} \text{sgn}(\theta).$$

The diffracted component, as expressed in (4) is exact at the shadow boundary ($v = 0$) and also for large values of v ($v > 2\pi$). The largest amplitude error occurs at $v = 0.75$ where the exact value is 0.3582, and the approximate value is 0.3622 which is a 1 percent error. The largest phase error occurs at $v = 1.0$ and 4.5, where the error is -2.2° and 2.2° respectively.

The total signal (direct + reflected + diffracted components) is given by

$$E(\theta) = E1(\theta) - E2(\theta) - E3(\theta) + E3(\theta - 2\alpha) + E3(-\theta - 2\beta) - E3(-\theta - 2\alpha - 2\beta). \quad (5)$$

The power density,

$$P(\theta) = \frac{(P)(G)}{4\pi(D1 + D2)^2} |E^2(\theta)|. \quad (6)$$

If the transmitter and the receiver are on opposite sides of the wedge apex, are near the wedge surface, $\alpha + \beta < \pi/8$ and $v > 2\pi$, then a simple expression can be derived for the power density.

$$P(HT, HR) = (P)(G) \frac{4\pi}{\lambda^2} \left(\frac{HT}{D1 + D2} \right)^2 \cdot \left(\frac{HR}{D1 + D2} \right)^2 \frac{1}{\pi^4} \left(\frac{\sqrt{\lambda/D}}{\alpha + \beta} \right)^6 \quad (7)$$

where

HT = height of transmitter above wedge surface

HR = height of receiver above wedge surface.

A well-known expression for power density for the case of flat ground, and the transmitter and receiver near ground level, is given by

$$P_{FG}(HT, HR) = (P)(G) \frac{4\pi}{\lambda^2} \left(\frac{HT}{D1 + D2} \right)^2 \cdot \left(\frac{HR}{D1 + D2} \right)^2. \quad (8)$$

This equation is valid if $(HT)(HR) < (D1 + D2)\lambda/8$. A comparison of the two equations shows that the dependence on transmitter and receiver heights above the wedge surface and distance $(D1 + D2)$ is the same as that of flat ground. If the transmitter or receiver height is doubled, then the signal level increases by 6 dB. The ratio of $P(HT, HR)/P_{FG}(HT, HR)$ is defined as the wedge attenuation and is given by

$$WA = \frac{1}{\pi^4} \left(\frac{\sqrt{\lambda/D}}{\alpha + \beta} \right)^6. \quad (9)$$

Equation (9) can be used to determine the attenuation caused by a hump relative to the flat runway case. Equation (9) is plotted in Fig. 3 as attenuation (dB = 10 log (1/WA)) versus

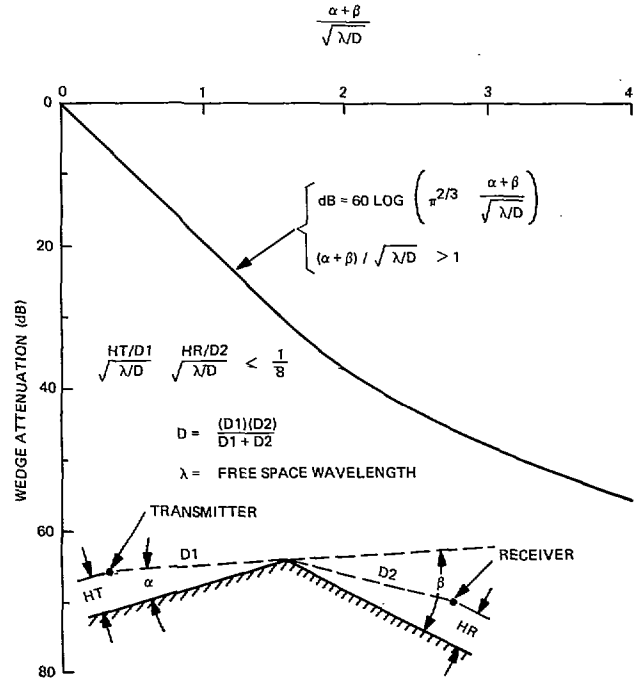


Fig. 3. Wedge attenuation (with respect to the reference case of flat ground) versus wedge angle.

normalized wedge angle for $(\alpha + \beta)/\sqrt{\lambda/D} > 1$. By definition, the wedge attenuation is 0 dB when the wedge angle is equal to zero. The attenuation for $(\alpha + \beta)/\sqrt{\lambda/D}$ between 0 and 1 was determined by evaluating (6).

Equations (1)-(6) have been used to compute the power density at several runways. The results of some of these computations, along with comparisons to measured results, are presented in the following sections. Appendix I presents a computer program, written in Basic, in which receiver position is an input and power density is the output. A simple and helpful method for modeling a runway hump is to use the threshold and stop end points plus one other point on the runway centerline to define the wedge geometry.

IV. OTTAWA INTERNATIONAL AIRPORT, RUNWAY 14

The results of computations of the MLS (C-band) power density along the approach to Runway 14 at Ottawa International Airport, Canada, are shown in Figs. 4, 5, and 6. The assumed runway profile is shown as a cross hatched sector.

The measured data shown in Fig. 4 was taken by means of a helicopter flying approximately 8 ft above the runway centerline [12]. The power measurements were not calibrated. Consequently, for comparison purposes the level of the measured curve was adjusted for a best fit in the runway segment closest to the azimuth transmitter where the flat ground model is valid. The comparison shows that the trend of computed and measured data is the same. At Ottawa Runway 14 there is significant multipath in the shadow region, which may explain some of the differences in that region. The best comparison should be with respect to data measured using a stationary vehicle along the runway centerline with a stable directional receive antenna of known gain. Measurements of this type are described in the following section.

The computed power density for a centerline approach to

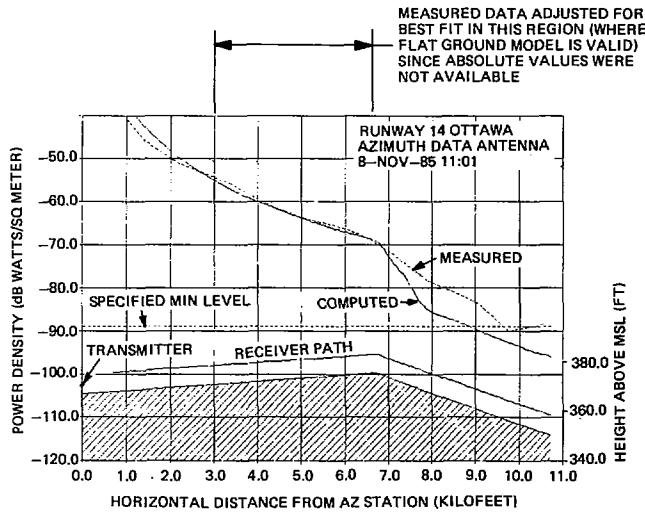


Fig. 4. Ottawa runway 14, computed power density, antenna phase center at 370 ft MSL.

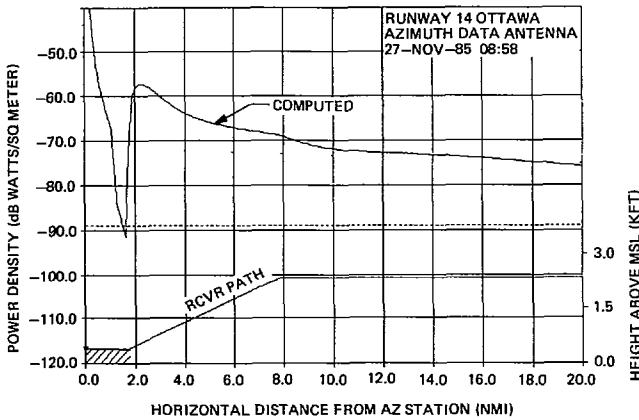


Fig. 5. Ottawa runway 14, computed power density, antenna phase center at 370 ft MSL, 20 NM range.

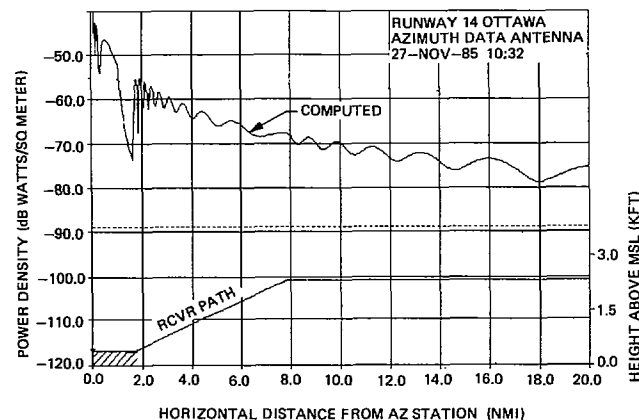


Fig. 6. Ottawa runway 14, computed power density, antenna phase center at 390 ft MSL, 20 NM range.

Ottawa Runway 14, starting at 20 NM, is shown in Fig. 5. It is noted that near touchdown the power density level is below the specified minimum level. Fig. 6 shows the same approach with the transmitting antenna raised 20 ft. For this case the power density level is well above the requirement.

V. BEDFORD U.K. RUNWAY 27

Absolute C-band measurements relative to free-space loss were made in 1973 by the United Kingdom Royal Aircraft Establishment (UKRAE) [4] (see Fig. 7). The free-space loss (FSL) factor is given by

$$FSL = \left(\frac{\lambda}{4\pi R} \right)^2 \tag{10}$$

where

R = distance from transmitter to receiver.

Free-space loss is related to power density, PD, by

$$PD = (P)(G)(FSL) \frac{(4\pi)}{\lambda^2} \tag{11}$$

This expression is used to convert the RAE measurements to power density.

The Bedford U.K. Runway 27 centerline profile and the assumed wedge surface is shown in Fig. 7. (It is noted that for distances less than 3000 ft, a steeper wedge angle would be a better approximation.) The computed and measured results for a transmitter located 1 ft above the wedge surface is presented in Fig. 8. The results for a transmitter located 4.8 ft above the wedge surface is presented in Fig. 9.

More recent measurements (March 1986) [13] have been obtained for an actual MLS installed on Runway 27. This data is summarized in Fig. 10. The measurements were made using a calibrated spectrum analyzer, a receive antenna with 20.4 dBi gain and a cable with 10.0 dB loss. It is noted that the agreement between the simulations and measurements is quite good near the runway threshold.

It should be noted that for MLS an accurate estimate of power density along the runway surface away from the threshold is not of primary concern since the power increases inversely with the fourth power of distance (see (7)). The critical point is the aircraft touch down point near the threshold, where the power density is at a minimum value. It is believed that in almost all cases the single-wedge model presented in this paper will provide an accurate estimate (within ± 3 dB) near the threshold. If desired, at some runways such as Bedford Runway 27, the accuracy at shorter distances can be improved by adjusting the wedge geometry as a function of receiver distance or by using a multiple wedge model as described in [5].

VI. CONCLUSION

This paper has presented a theoretical model for estimating the power densities of signals from a microwave landing system along the approach path of an aircraft and during rollout for the humped runway situation. It should provide fairly accurate estimates of the absolute power densities for the angle guidance and distance measuring signals. It is believed that near the threshold the prediction accuracy can be within ± 3 dB for the angle guidance equipment. Although there is no experimental data for the distance measuring equipment, it is believed that the prediction accuracy should be within the same limits. The computations are made using simple func-

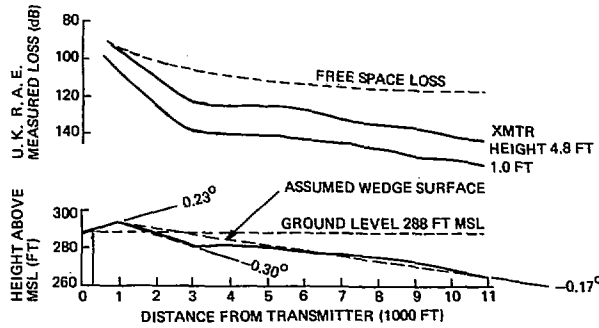


Fig. 7. Bedford U.K. main runway centerline profile and U.K.R.A.E. measurements.

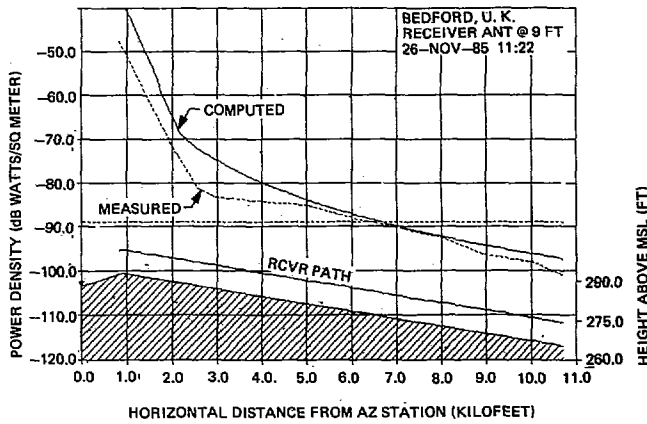


Fig. 8. Bedford U.K. runway 27, computed power density, antenna phase center at 289 ft MSL.

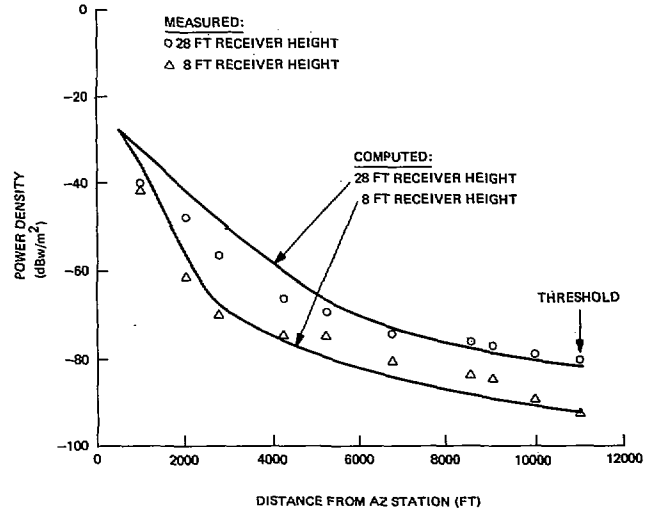


Fig. 10. Bedford U.K. runway 27, MLS installation, computed power density, wedge angles 0.23° and -0.17°, apex at 1230 ft, data antenna height above wedge surface is 2 ft.

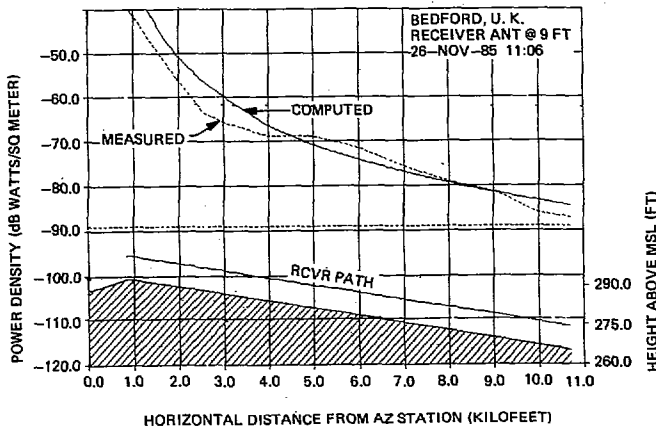


Fig. 9. Bedford U.K. runway 27, computed power density, antenna phase center at 292.8 ft MSL.

tions which approximate the antenna vertical plane patterns and the diffraction coefficients.

APPENDIX I

Computer Program Name: HUMPRWY
Language: BASIC

Input Data:

ZT = height of transmitter (ft)

- Z1 = height of wedge surface directly below the transmitter (ft)
- X2 = position (X coordinate) of wedge apex (ft)
- Z2 = height of wedge apex (ft)
- X3 = position (X coordinate) of a point on the wedge surface beyond the apex (ft)
- Z3 = height of same point (ft)
- WL = wavelength (0.2 ft for AGE, 1.0 ft for DME)
- DBW = P (13 dBW for AGE, 18 dBW for DME)
- DBG = G (8 dBi for AGE, 4dBi for DME)
- VPF = vertical pattern factor (1.215 for AGE, 0.30 for DME)
- XR = position (X coordinate) of receiver (ft)
- ZR = height of receiver (ft)

NOTE:

- AGE = angle guidance equipment
- DME = distance measuring equipment

Output Data:

DBWM2 = power density (dBW/m²)

Listing:

```

100 DATA 2,0,1230,5,9000,-18,.2,13,8,1.215
110 READ ZT,Z1,X2,Z2,X3,Z3,WL,DBW,DBG,VPF
120 INPUT "RECEIVER COORDINATES X,Z = ";XR,ZR
130 PI=4*ATN(1)
140 THETA1=ATN((Z2-ZT)/X2)
150 D2=SQR((ZR-Z2)^2+(XR-X2)^2);D1=SQR((Z2-ZT)^2+X2^2)
160 D3=SQR((ZR-ZT)^2+XR^2)
170 ALPHA=ATN((Z2-Z1)/X2)-THETA1
180 BETA=ATN((Z2-Z3)/(X3-X2))+THETA1
190 ZI=Z2-D1*SIN(2*ALPHA+THETA1);XI=X2-D1*COS(2*ALPHA+THETA1)
200 ZI2=Z2+D1*SIN(2*BETA-THETA1);XI2=X2-D1*COS(2*BETA-THETA1)
210 D4=SQR((ZR-ZI)^2+(XR-XI)^2)
220 D5=SQR((ZR-ZI2)^2+(XR-XI2)^2)
230 PHE=ATN((ZR-ZT)/XR)-THETA1
240 IF XR>X2 THEN GAMMA=ATN((ZR-Z2)/(XR-X2))
250 IF XR<X2 THEN GAMMA=ATN((ZR-Z2)/(XR-X2))+PI
260 IF XR=X2 THEN GAMMA=PI/2
270 THETA=GAMMA-THETA1
280 W=VPF*PHE*45/ATN(1);GOSUB 650;V1=1+.8*TANH
290 PHE2=ATN((ZR-ZI)/(XR-XI))-THETA1-2*ALPHA
300 PHE3=ATN((ZR-ZI2)/(XR-XI2))+2*BETA-THETA1
310 W=VPF*PHE2*45/ATN(1);GOSUB 650;V2=1-.8*TANH
320 W=VPF*PHE3*45/ATN(1);GOSUB 650;V3=1-.8*TANH
330 D3P=D1*2*(SIN(PHE/2))^2+D2*2*(SIN((THETA-PHE)/2))^2
340 D4P=D1*2*(SIN(PHE2/2))^2+D2*2*(SIN((THETA-2*ALPHA-PHE2)/2))^2
350 D5P=D1*2*(SIN(PHE3/2))^2+D2*2*(SIN((THETA+2*BETA-PHE3)/2))^2
360 SN1=SGN(THETA);IF SN1=0 THEN SN1=1
370 SN2=SGN(THETA-2*ALPHA);IF SN2=0 THEN SN2=1
380 SN3=SGN(-THETA-2*BETA);IF SN3=0 THEN SN3=1
390 SN4=SGN(-THETA-2*ALPHA-2*BETA);IF SN4=0 THEN SN4=1
400 E1R=(D1+D2)*V1*(.5+.5*SN1)*COS(2*PI*D3P/WL)/D3
410 E1I=(D1+D2)*V1*(.5+.5*SN1)*SIN(2*PI*D3P/WL)/D3
420 E2R=(D1+D2)*V2*(.5+.5*SN2)*COS(2*PI*D4P/WL)/D4
430 E2I=(D1+D2)*V2*(.5+.5*SN2)*SIN(2*PI*D4P/WL)/D4
440 E3R=(D1+D2)*V3*(.5+.5*SN3)*COS(2*PI*D5P/WL)/D5
450 E3I=(D1+D2)*V3*(.5+.5*SN3)*SIN(2*PI*D5P/WL)/D5
460 D=D1*D2/(D1+D2)
470 FOR K= 1 TO 4
480 IF K=1 THEN THET=THETA;SN=SN1;GOTO 520
490 IF K=2 THEN THET=THETA-2*ALPHA;SN=SN2;GOTO 520
500 IF K=3 THEN THET=-THETA-2*BETA;SN=SN3;GOTO 520
510 IF K=4 THEN THET=-THETA-2*ALPHA-2*BETA;SN=SN4
520 V=2*PI*SQR(D/WL)*SIN(THET/2);V=ABS(V)
530 IF V=0 THEN E3R(K)=.5;E3I(K)=0;GOTO 580
540 W=V;GOSUB 650;TANH1=TANH
550 W=V/2.4;GOSUB 650;TANH2=TANH
560 E3R(K)=(TANH1/2/V-V*EXP(-1.5*V)/4)*SN*COS(PI*TANH2/4)
570 E3I(K)=(TANH1/2/V-V*EXP(-1.5*V)/4)*SN*SIN(-PI*TANH2/4)
580 NEXT K
590 ER=E1R-E2R-E3R-E3R(1)+E3R(2)+E3R(3)-E3R(4)
600 EI=E1I-E2I-E3I-E3I(1)+E3I(2)+E3I(3)-E3I(4)
610 P=(ER^2+EI^2)/4/PI/(D1+D2)^2
620 IF P=0 THEN DBP=-1000 ELSE DBP=10*LOG(P)/LOG(10)
630 DBWM2=DBP+DBW+DBG+10.3
640 PRINT "X = "XR,"Z = "ZR,"DB W/M^2 = "DBWM2;END
650 IF W>10 THEN TANH=1;GOTO 680
660 IF W<-10 THEN TANH=-1;GOTO 680
670 TANH=(EXP(W)-EXP(-W))/(EXP(W)+EXP(-W))
680 RETURN

```

Fig. 11.

ACKNOWLEDGMENT

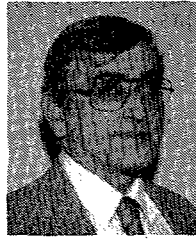
The methodology presented in this paper has evolved during the many years of the design, development, and implementation of the microwave landing system. The author wishes to thank the Federal Aviation Administration and the MLS community for their help with the definition and understanding of the problem. The experimental data provided by Mr. Jim Hastie of the Canadian Ministry of Transportation and Mr. Pat Neilan of the United Kingdom Civil Aviation Authority, and the help provided by Mr. Allan Axel of Hazeltine Corporation with the analysis and computations are much appreciated.

Thanks are also given to Mrs. Dorothy Stark for her effort in preparing the manuscript.

REFERENCES

- [1] H. S. Carslaw, "Diffraction of waves by a wedge of any angle," *Proc. Lond. Math. Soc.*, vol. 18, pp. 291-306, 1919.
- [2] J. Capon, "Multipath parameter computations for the MLS simulation computer program," Lincoln Lab. Rep. FAA-RD-76-55, Project Rep. ATC-68, April 1976.
- [3] J. R. Wait and A. M. Conda, "Diffraction of electromagnetic waves by smooth obstacles for grazing angles," *J. Res. Nat. Bur. Stand. Radio Propagat.*, vol. 63D, no. 2, pp. 181-197, Sept. 1959.
- [4] J. Benjamin and G. E. J. Peake, "Contributions to the U. K. microwave landing system study (phase 1)," Royal Aircraft Establish-

- ment, Tech. Memo RAD 1021, May 1973.
- [5] R. Luebbers, V. Ungvichian, and L. Mitchell, "GTD terrain reflection model applied to ILS glide slope," *IEEE Trans. Aerosp. Electron. Syst.*, vol. AES-18, p. 11, Jan. 1982.
- [6] K. Chamberlin and R. J. Luebbers, "An evaluation of Longley-Rice and GTD propagation models," *IEEE Trans. Antennas Propagat.*, vol. AP-30, p. 1093, Nov. 1982.
- [7] R. J. Luebbers, "Finite conductivity uniform GTD versus knife edge diffraction of propagation path loss," *IEEE Trans. Antennas Propagat.*, vol. AP-32, Jan. 1984.
- [8] L. B. Felsen and N. Maruvitz, *Radiation and Scattering of Waves*. Englewood Cliffs, NJ: Prentice-Hall, 1973, sec. 6.3.
- [9] H. W. Redlien, R. J. Kelly, and J. L. Shagena, "Landing aircraft under poor conditions," *IEEE Spectrum*, vol. 15, pp. 52-57, Nov. 9, 1978.
- [10] A. R. Lopez, "Sharp cutoff radiation patterns," *IEEE Trans. Antennas Propagat.*, vol. AP-27, pp. 820-824, Nov. 1979.
- [11] —, "The geometrical theory of diffraction applied to antenna pattern and impedance calculations," *IEEE Trans. Antennas Propagat.*, vol. AP-14, pp. 40-45, Jan. 1966.
- [12] J. Hastie, private correspondence, measurements at Ottawa airport, Aug. 1985.
- [13] P. J. Neilan, private correspondence, measurements at U.K. Bedford Airport, May 1986.



Alfred R. Lopez (S'56-M'59-SM'69-F'83) was born in New York, NY, on November 10, 1930. He received the B.E.E. degree from Manhattan College, Riverdale, NY, in 1958, and the M.S.E.E. degree from the Polytechnic Institute of Brooklyn, Brooklyn, NY, in 1963.

In 1958 he joined Wheeler Laboratories Inc. which is now part of the Hazeltine Corporation Research Laboratories. He is currently a Senior Consulting Engineer for Hazeltine's Navigational Aids Systems group. His experience includes work on satellite, missile, aircraft and ground-based antennas. Since 1970 he has worked on the design and development of the microwave landing system and is recognized internationally for his technical contributions.